

The Path to N3LO Parton Distribution Functions

Phenomenology of Particle Physics Seminar — Max Planck Institute for Physics

Emanuele R. Nocera

Università degli Studi di Torino and INFN, Torino

17 April 2024



UNIVERSITÀ
DI TORINO

1. Parton Distribution Functions at the LHC

Determining PDFs from experimental data

- 1 Collinear, leading-twist factorisation of physical observables

$$\sigma(Q^2, \tau, \mathbf{k}) = \sum_{ij} \int_{\tau}^1 \frac{dz}{z} \mathcal{L}_{ij}(z, Q^2) \hat{\sigma}_{ij} \left(\frac{\tau}{z}, \alpha_s(Q^2), \mathbf{k} \right) \quad \mathcal{L}_{ij}(z, Q^2) = (f_i^{h1} \otimes f_j^{h2})(z, Q^2)$$

- 2 Parametrisation: general, smooth, flexible at an initial scale Q_0^2

$$x f_i(x, Q_0^2) = A_{f_i} x^{a_{f_i}} (1-x)^{b_{f_i}} \mathcal{F}(x, \{c_{f_i}\})$$

small x
large x

$$x f_i(x, Q^2) \xrightarrow{x \rightarrow 0} x^{a_{f_i}} \quad \xrightarrow[\text{smooth interpolation in between}]{\mathcal{F}(x, \{c_{f_i}\}) \xrightarrow[x \rightarrow 1]{x \rightarrow 0} \text{finite}} \quad x f_i(x, Q^2) \xrightarrow{x \rightarrow 1} (1-x)^{b_{f_i}}$$

(Regge theory)
(polynomials, neural networks)
(quark counting rules)

- 3 A prescription to determine/compute expectation values and uncertainties

$$\chi^2 = \sum_{i,j}^{N_{\text{dat}}} [T_i[\{\vec{a}\}] - D_i] (\text{cov}^{-1})_{ij} [T_j[\{\vec{a}\}] - D_j]$$

$$E[\mathcal{O}] = \int \mathcal{D}f \mathcal{P}(f|data) \mathcal{O}(f) \quad V[\mathcal{O}] = \int \mathcal{D}f \mathcal{P}(f|data) [\mathcal{O}(f) - E[\mathcal{O}]]^2$$

Monte Carlo: $\mathcal{P}(f|data) \rightarrow \{f_k\}$

Maximum likelihood: $\mathcal{P}(f|data) \rightarrow f_0$

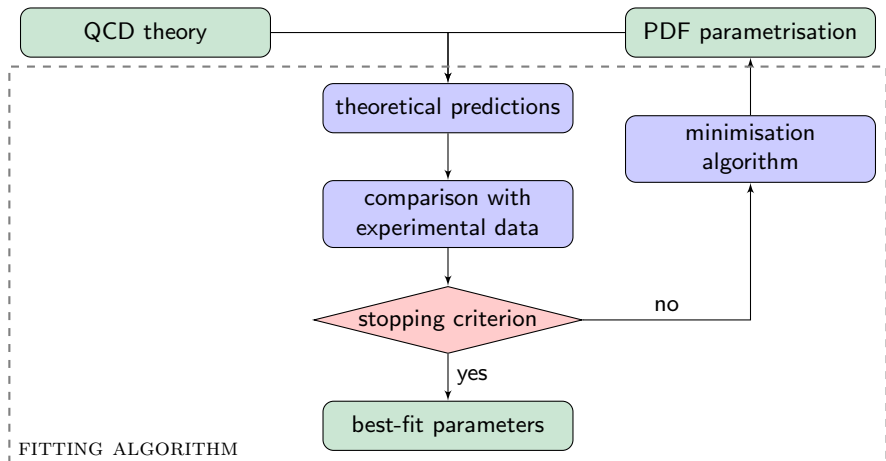
$$E[\mathcal{O}] \approx \frac{1}{N} \sum_k \mathcal{O}(f_k)$$

$$E[\mathcal{O}] \approx \mathcal{O}(f_0)$$

$$V[\mathcal{O}] \approx \frac{1}{N} \sum_k [\mathcal{O}(f_k) - E[\mathcal{O}]]^2$$

$$V[\mathcal{O}] \approx \text{Hessian}, \Delta\chi^2 \text{ envelope}, \dots$$

Determining PDFs from experimental data



Assume a reasonable PDF parametrisation

Obtain theoretical predictions for various processes and compare predictions to data

Determine the best-fit parameters via minimisation of a proper figure of merit (e.g. χ^2)

Self-validate PDF's accuracy and precision

Making predictions with PDFs

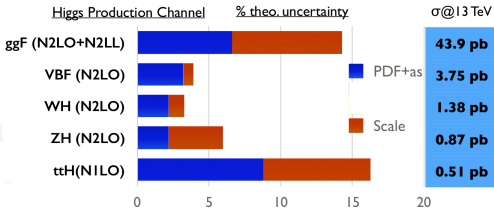
PDF uncertainty is often the dominant source of uncertainty in LHC cross sections

Higgs boson characterisation

Determination of SM parameters, such as the mass of the W boson

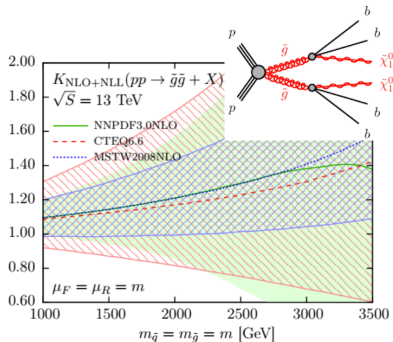
Searches for beyond SM physics at large invariant mass of the final state

Precision



| Channel | $m_{W^+} - m_{W^-}$ [MeV] | Stat. Unc. | Muon Unc. | Elec. Unc. | Recoil Unc. | Bckg. Unc. | QCD Unc. | EW Unc. | PDF Unc. | Total Unc. |
|------------------------|---------------------------|------------|-----------|------------|-------------|------------|----------|---------|----------|------------|
| $W \rightarrow e\nu$ | -29.7 | 17.5 | 0.0 | 4.9 | 0.9 | 5.4 | 0.5 | 0.0 | 24.1 | 30.7 |
| $W \rightarrow \mu\nu$ | -28.6 | 16.3 | 11.7 | 0.0 | 1.1 | 5.0 | 0.4 | 0.0 | 26.0 | 33.2 |
| Combined | -29.2 | 12.8 | 3.3 | 4.1 | 1.0 | 4.5 | 0.4 | 0.0 | 23.9 | 28.0 |

Discovery



[Plot from the CERN Yellow Report 2016]

[EPJC 76 (2016) 53]

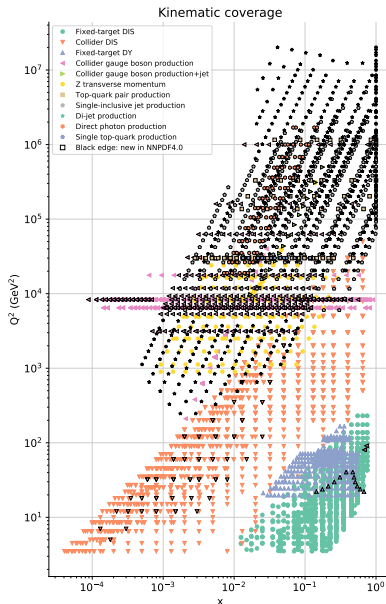
Next generation PDFs: NNPDF4.0 [EPJ C82 (2022) 428]

- Refined theoretical framework [EPJ C79 (2019) 282; EPJ C81 (2021) 37; EPJ C80 (2020) 1168]
 - nuclear uncertainties for both deuteron and heavy nuclei included by default
 - NNLO charm-quark massive corrections implemented
 - EW corrections not included to ensure consistency with data, but carefully checked
 - charm PDF parametrised on the same footing as other PDFs
- Improved implementation of PDF properties [JHEP 11 (2020) 129]
 - extended positivity constraints for light quark/antiquark and gluon PDFs
 - extended integrability constraints of non-singlet light quark PDF combinations
- New PDF parametrisation and optimisation [EPJ C79 (2019) 676]
 - single neural network to parametrise eight independent PDF combinations
 - check of the independence of the results from the chosen parametrisation basis
 - new optimisation strategy based on gradient descent rather than genetic algorithms
 - scan of the hyperparameter space to find the optimal minimisation settings
- Complete statistical validation of PDF uncertainties [Acta Phys. Polon. B52 (2021) 243]
 - (multi-)closure tests to validate PDF uncertainties in the data region
 - future tests to check the sensibleness of PDF uncertainties in extrapolation regions
- Open source fitting code [EPJ C 81 (2021) 958]

<https://nnpdf.mi.infn.it/nnpdf-open-source-code/>

Next generation PDFs: NNPDF4.0 [EPJ C82 (2022) 428]

| Data set | N_{dat} | χ^2/N_{dat} |
|--------------------------|------------------|-------------------------|
| Fixed-target DIS | 1881 | 1.10 |
| HERA | 1208 | 1.21 |
| σ_c | 37 | 2.11 |
| σ_b | 26 | 1.48 |
| Fixed-target Drell-Yan | 189 | 1.00 |
| CDF | 28 | 1.31 |
| D0 | 37 | 1.00 |
| ATLAS | 621 | 1.18 |
| Drell-Yan, 7, 8, 13 TeV | 153 | 1.32 |
| W +jet, 8 TeV | 32 | 1.15 |
| single top, 7, 8, 13 TeV | 14 | 0.36 |
| di-jets, 7 TeV | 90 | 1.93 |
| jets, 8 TeV | 171 | 0.61 |
| top pair, 7, 8, 13 TeV | 16 | 2.30 |
| Zp_T , 8 TeV | 92 | 0.86 |
| direct photon, 13 TeV | 53 | 0.72 |
| CMS | 411 | 1.40 |
| Drell-Yan, 7, 8 TeV | 154 | 1.34 |
| single top, 7, 8, 13 TeV | 3 | 0.43 |
| di-jets, 7 TeV | 54 | 1.67 |
| di-jets, 8 TeV | 122 | 1.50 |
| top pair, 5, 7, 8 TeV | 29 | 0.84 |
| top pair, 13 TeV | 21 | 0.67 |
| Zp_T , 8 TeV | 28 | 1.42 |
| LHCb | 116 | 1.53 |
| Total | 4491 | 1.17 |

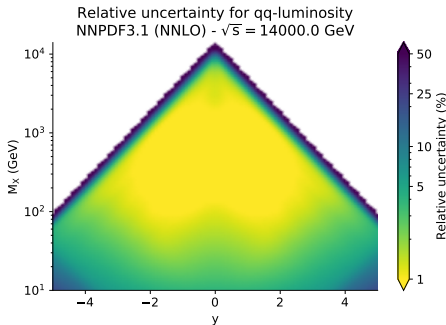


So, how large are PDF uncertainties?

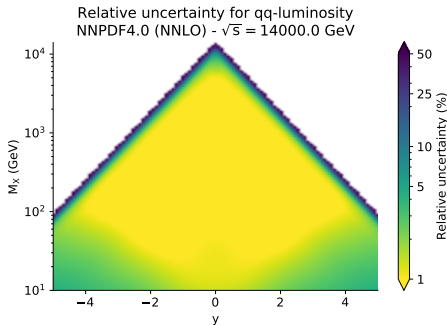
$$\mathcal{L}_{ij}(M_X, y, \sqrt{s}) = \frac{1}{s} f_i \left(\frac{M_X e^y}{\sqrt{s}}, M_X \right) f_j \left(\frac{M_X e^{-y}}{\sqrt{s}}, M_X \right)$$

SINGLET

NNPDF3.1 (NNLO)



NNPDF4.0 (NNLO)



Steady progress towards 1% relative uncertainties on \mathcal{L}_{ij} in a broad kinematic range

The path towards 1% PDF uncertainties goes through data, methodology and theory

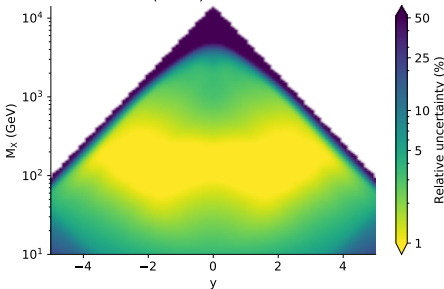
So, how large are PDF uncertainties?

$$\mathcal{L}_{ij}(M_X, y, \sqrt{s}) = \frac{1}{s} f_i \left(\frac{M_X e^y}{\sqrt{s}}, M_X \right) f_j \left(\frac{M_X e^{-y}}{\sqrt{s}}, M_X \right)$$

SINGLET

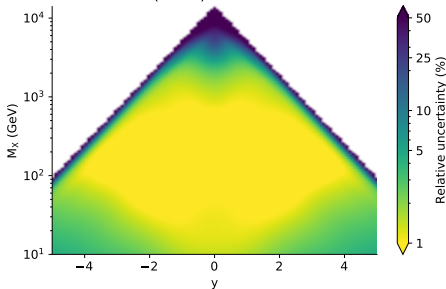
NNPDF3.1 (NNLO)

Relative uncertainty for $q\bar{q}$ -luminosity
NNPDF3.1 (NNLO) - $\sqrt{s} = 14000.0$ GeV



NNPDF4.0 (NNLO)

Relative uncertainty for $q\bar{q}$ -luminosity
NNPDF4.0 (NNLO) - $\sqrt{s} = 14000.0$ GeV



Steady progress towards 1% relative uncertainties on \mathcal{L}_{ij} in a broad kinematic range

The path towards 1% PDF uncertainties goes through data, methodology and theory

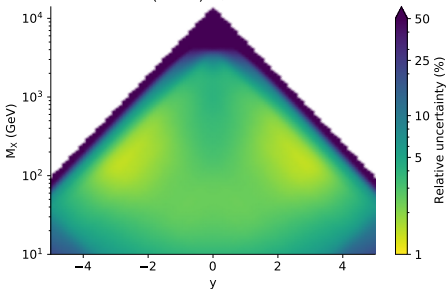
So, how large are PDF uncertainties?

$$\mathcal{L}_{ij}(M_X, y, \sqrt{s}) = \frac{1}{s} f_i \left(\frac{M_X e^y}{\sqrt{s}}, M_X \right) f_j \left(\frac{M_X e^{-y}}{\sqrt{s}}, M_X \right)$$

FLAVOURS

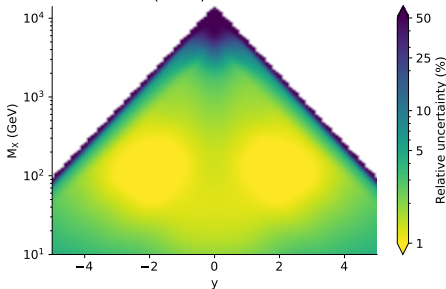
NNPDF3.1 (NNLO)

Relative uncertainty for $u\bar{d}$ -luminosity
NNPDF3.1 (NNLO) - $\sqrt{s} = 14000.0$ GeV



NNPDF4.0 (NNLO)

Relative uncertainty for $u\bar{d}$ -luminosity
NNPDF4.0 (NNLO) - $\sqrt{s} = 14000.0$ GeV



Steady progress towards 1% relative uncertainties on \mathcal{L}_{ij} in a broad kinematic range

The path towards 1% PDF uncertainties goes through data, methodology and theory

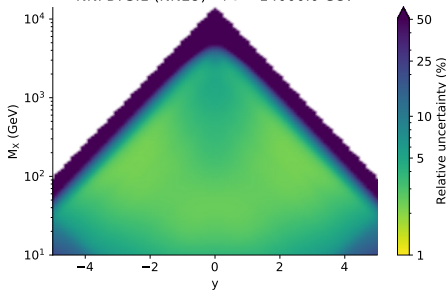
So, how large are PDF uncertainties?

$$\mathcal{L}_{ij}(M_X, y, \sqrt{s}) = \frac{1}{s} f_i \left(\frac{M_X e^y}{\sqrt{s}}, M_X \right) f_j \left(\frac{M_X e^{-y}}{\sqrt{s}}, M_X \right)$$

FLAVOURS

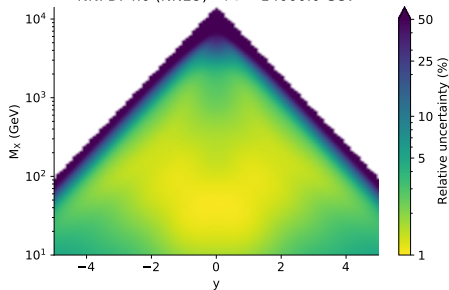
NNPDF3.1 (NNLO)

Relative uncertainty for $d\bar{u}$ -luminosity
NNPDF3.1 (NNLO) - $\sqrt{s} = 14000.0$ GeV



NNPDF4.0 (NNLO)

Relative uncertainty for $d\bar{u}$ -luminosity
NNPDF4.0 (NNLO) - $\sqrt{s} = 14000.0$ GeV



Steady progress towards 1% relative uncertainties on \mathcal{L}_{ij} in a broad kinematic range

The path towards 1% PDF uncertainties goes through data, methodology and theory

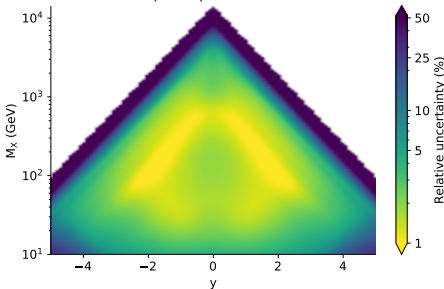
So, how large are PDF uncertainties?

$$\mathcal{L}_{ij}(M_X, y, \sqrt{s}) = \frac{1}{s} f_i \left(\frac{M_X e^y}{\sqrt{s}}, M_X \right) f_j \left(\frac{M_X e^{-y}}{\sqrt{s}}, M_X \right)$$

GLUON

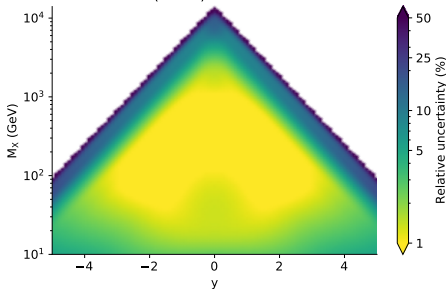
NNPDF3.1 (NNLO)

Relative uncertainty for gg-luminosity
NNPDF3.1 (NNLO) - $\sqrt{s} = 14000.0$ GeV



NNPDF4.0 (NNLO)

Relative uncertainty for gg-luminosity
NNPDF4.0 (NNLO) - $\sqrt{s} = 14000.0$ GeV



Steady progress towards 1% relative uncertainties on \mathcal{L}_{ij} in a broad kinematic range

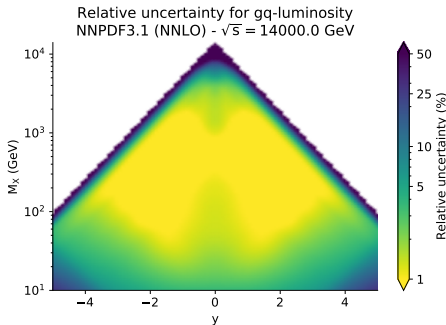
The path towards 1% PDF uncertainties goes through data, methodology and theory

So, how large are PDF uncertainties?

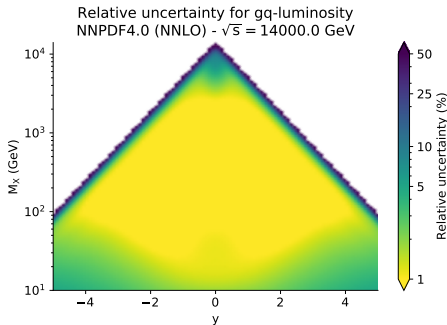
$$\mathcal{L}_{ij}(M_X, y, \sqrt{s}) = \frac{1}{s} f_i \left(\frac{M_X e^y}{\sqrt{s}}, M_X \right) f_j \left(\frac{M_X e^{-y}}{\sqrt{s}}, M_X \right)$$

GLUON

NNPDF3.1 (NNLO)



NNPDF4.0 (NNLO)



Steady progress towards 1% relative uncertainties on \mathcal{L}_{ij} in a broad kinematic range

The path towards 1% PDF uncertainties goes through data, methodology and theory

2. Theory uncertainties in PDF determination

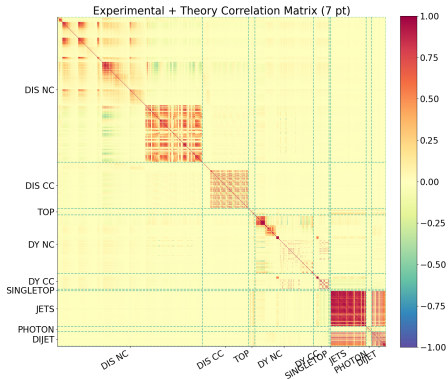
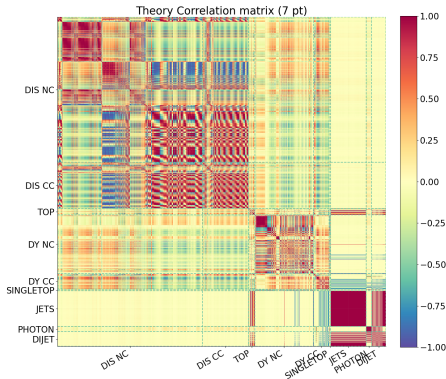
Theory uncertainties in PDF determination

Assuming that theory uncertainties are (a) Gaussian and (b) independent from experimental uncertainties, modify the figure of merit to account for theory errors

$$\chi^2 = \sum_{i,j}^{N_{\text{dat}}} (D_i - T_i)(\text{cov}_{\text{exp}} + \text{cov}_{\text{th}})^{-1}_{ij} (D_j - T_j); \quad (\text{cov}_{\text{th}})_{ij} = \frac{1}{N} \sum_k \Delta_i^{(k)} \Delta_j^{(k)}; \quad \Delta_i^{(k)} \equiv T_i^{(k)} - T_i$$

Problem reduced to estimate the th. cov. matrix, e.g. in terms of nuisance parameters

$$\Delta_i^{(k)} = T_i(\mu_R, \mu_F) - T_i(\mu_{R,0}, \mu_{F,0}); \quad \text{vary scales in } \frac{1}{2} \leq \frac{\mu_F}{\mu_{F,0}}, \frac{\mu_R}{\mu_{R,0}} \leq 2$$



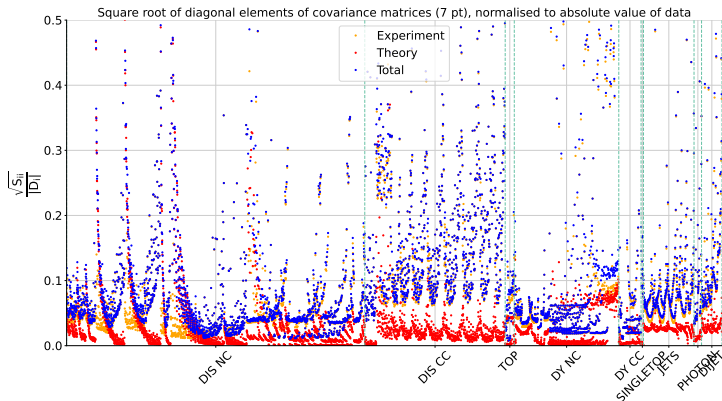
Theory uncertainties in PDF determination

Assuming that theory uncertainties are (a) Gaussian and (b) independent from experimental uncertainties, modify the figure of merit to account for theory errors

$$\chi^2 = \sum_{i,j}^{N_{\text{dat}}} (D_i - T_i) (\text{cov}_{\text{exp}} + \text{cov}_{\text{th}})^{-1}_{ij} (D_j - T_j); \quad (\text{cov}_{\text{th}})_{ij} = \frac{1}{N} \sum_k \Delta_i^{(k)} \Delta_j^{(k)}; \quad \Delta_i^{(k)} \equiv T_i^{(k)} - T_i$$

Problem reduced to estimate the th. cov. matrix, e.g. in terms of nuisance parameters

$$\Delta_i^{(k)} = T_i(\mu_R, \mu_F) - T_i(\mu_{R,0}, \mu_{F,0}); \quad \text{vary scales in } \frac{1}{2} \leq \frac{\mu_F}{\mu_{F,0}}, \frac{\mu_R}{\mu_{R,0}} \leq 2$$



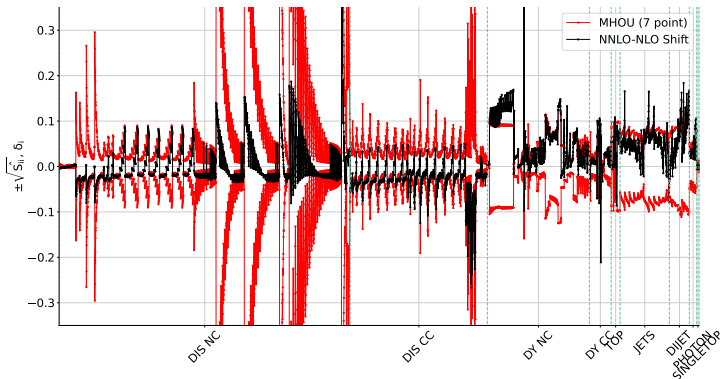
Theory uncertainties in PDF determination

Assuming that theory uncertainties are (a) Gaussian and (b) independent from experimental uncertainties, modify the figure of merit to account for theory errors

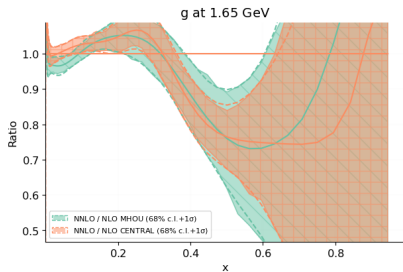
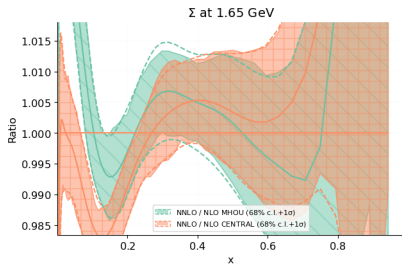
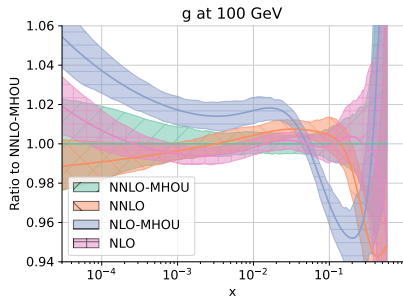
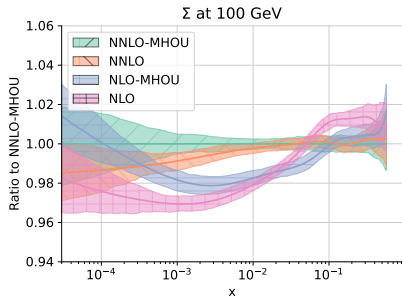
$$\chi^2 = \sum_{i,j}^{N_{\text{dat}}} (D_i - T_i)(\text{cov}_{\text{exp}} + \text{cov}_{\text{th}})^{-1}_{ij} (D_j - T_j); \quad (\text{cov}_{\text{th}})_{ij} = \frac{1}{N} \sum_k^N \Delta_i^{(k)} \Delta_j^{(k)}; \quad \Delta_i^{(k)} \equiv T_i^{(k)} - T_i$$

Problem reduced to estimate the th. cov. matrix, e.g. in terms of nuisance parameters

$$\Delta_i^{(k)} = T_i(\mu_R, \mu_F) - T_i(\mu_{R,0}, \mu_{F,0}); \quad \text{vary scales in } \frac{1}{2} \leq \frac{\mu_F}{\mu_{F,0}}, \frac{\mu_R}{\mu_{R,0}} \leq 2$$



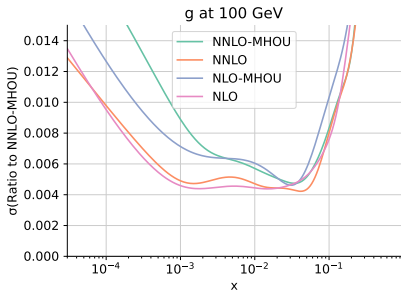
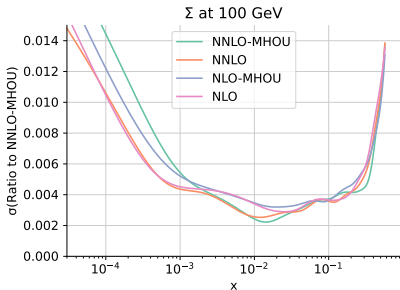
Theory uncertainties in PDF determination



Faster perturbative convergence when MHOU are incorporated into PDFs

[EPJ C79 (2019) 838; *ibid.* 931; arXiv:2401.10319]

Theory uncertainties in PDF determination



| Dataset | N_{dat} | NLO | | NNLO | |
|-----------------------|------------------|-------------|-------------|-------------|-------------|
| | | no MHOU | MHOU | no MHOU | MHOU |
| DIS NC | 2100 | 1.30 | 1.22 | 1.23 | 1.20 |
| DIS CC | 989 | 0.92 | 0.87 | 0.90 | 0.90 |
| DY NC | 736 | 2.01 | 1.71 | 1.20 | 1.15 |
| DY CC | 157 | 1.48 | 1.42 | 1.48 | 1.37 |
| Top pairs | 64 | 2.08 | 1.24 | 1.21 | 1.43 |
| Single-inclusive jets | 356 | 0.84 | 0.82 | 0.96 | 0.81 |
| Dijets | 144 | 1.52 | 1.84 | 2.04 | 1.71 |
| Prompt photons | 53 | 0.59 | 0.49 | 0.75 | 0.67 |
| Single top | 17 | 0.36 | 0.35 | 0.36 | 0.38 |
| Total | 4616 | 1.34 | 1.23 | 1.17 | 1.13 |

Overall (rather small) variation of uncertainties. Tensions relieved: improvement in χ^2

[EPJ C79 (2019) 838; *ibid.* 931; arXiv:2401.10319]

3. N3LO QCD corrections in PDF determination

N³LO QCD corrections in PDF determination

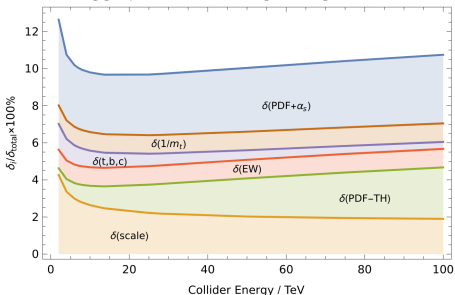
NNLO is the precision frontier for PDF determination

N3LO is the precision frontier for partonic cross sections

Mismatch between perturbative order of partonic cross sections and accuracy of PDFs may become a significant source of uncertainty

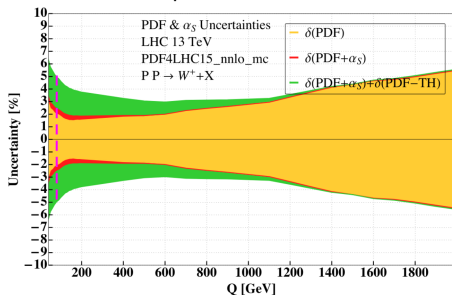
$$\hat{\sigma} = \alpha_s^p \hat{\sigma}_0 + \alpha_s^{p+1} \hat{\sigma}_1 + \alpha_s^{p+2} \hat{\sigma}_2 + \mathcal{O}(\alpha_s^{p+3}) \quad \delta(\text{PDF} - \text{TH}) = \frac{1}{2} \left| \frac{\sigma_{\text{NNLO-PDFs}}^{(2)} - \sigma_{\text{NLO-PDFs}}^{(2)}}{\sigma_{\text{NNLO-PDFs}}^{(2)}} \right|$$

Higgs production in gluon-gluon fusion



[CERN Yellow Rep. Monogr. 7 (2019) 221]

W⁺ boson production in CC Drell-Yan



[JHEP 11 (2020) 143]

N³LO QCD corrections in PDF determination

Splitting Functions (information is partial)

Singlet ($P_{qq}, P_{gg}, P_{gq}, P_{qg}$)

- large- n_f limit [NPB 915 (2017) 335; arXiv:2308.07958]
- small- x limit [JHEP 06 (2018) 145]
- large- x limit [NPB 832 (2010) 152; JHEP 04 (2020) 018; JHEP 09 (2022) 155]
- 5 (10) lowest Mellin moments [PLB 825 (2022) 136853; ibid. 842 (2023) 137944; ibid. 846 (2023) 138215]

Non-singlet ($P_{NS,v}, P_{NS,+}, P_{NS,-}$)

- large- n_f limit [NPB 915 (2017) 335; arXiv:2308.07958]
- small- x limit [JHEP 08 (2022) 135]
- large- x limit [JHEP 10 (2017) 041]
- 8 lowest Mellin moments [JHEP 06 (2018) 073]

DIS structure functions (F_L, F_2, F_3)

- DIS NC (massless) [NPB 492 (1997) 338; PLB 606 (2005) 123; NPB 724 (2005) 3]
- DIS CC (massless) [Nucl.Phys.B 813 (2009) 220]
- massive from parametrisation combining known limits and damping functions [NPB 864 (2012) 399]

PDF matching conditions

- all known except for $a_{H,g}^3$ [NPB 820 (2009) 417; NPB 886 (2014) 733; JHEP 12 (2022) 134]

Coefficient functions for other processes

- DY (inclusive) [JHEP 11 (2020) 143]; DY (y differential) [PRL 128 (2022) 052001]

Approximate N3LO anomalous dimensions

- We include all analytically known terms in the n_f expansion

$$\gamma_{ij}^{(3)}(N) = \gamma_{ij}^{(3,0)}(N) + n_f \gamma_{ij}^{(3,1)}(N) + n_f^2 \gamma_{ij}^{(3,2)}(N) + n_f^3 \gamma_{ij}^{(3,3)}(N),$$

which we collectively denote as $\gamma_{ij,n_f}^{(3)}(N)$.

- We include all analytically known terms from large- x and small- x resummation, to the highest known logarithmic accuracy, including all known subleading power corrections in both limits: $\gamma_{ij,N \rightarrow \infty}^{(3)}(N)$, $\gamma_{ij,N \rightarrow 0}^{(3)}(N)$, $\gamma_{ij,N \rightarrow 1}^{(3)}(N)$.
- We write the approximate anomalous dimension as

$$\gamma_{ij}^{(3)}(N) = \gamma_{ij,n_f}^{(3)}(N) + \gamma_{ij,N \rightarrow \infty}^{(3)}(N) + \gamma_{ij,N \rightarrow 0}^{(3)}(N) + \gamma_{ij,N \rightarrow 1}^{(3)}(N) + \tilde{\gamma}_{ij}^{(3)}(N).$$

- We determine $\tilde{\gamma}_{ij}^{(3)}(N)$ as a linear combination of a set of n^{ij} interpolating functions (equal to the number of known Mellin moments):
 $n_{ij} - n_H G_\ell^{ij}(N)$ (fixed) and $n_H H_\ell^{ij}(N)$ (varied)

$$\tilde{\gamma}_{ij}^{(3)}(N) = \sum_{\ell=1}^{n^{ij}-n_H} b_\ell^{ij} G_\ell^{ij}(N) + \sum_{\ell=1}^{n_H} b_{n^{ij}-2+\ell}^{ij} H_\ell^{ij}(N),$$

with the coefficients b_ℓ^{ij} constrained by Mellin moments.

- We make \tilde{N}_{ij} different choices for each of the $n_H = 2$ functions $H_\ell^{ij}(N)$ in the singlet sector; $n_H = 0$ in the non-singlet sector.

Incomplete Higher-Order Uncertainties

- We have an ensemble of \tilde{N}_{ij} different approximations to $\gamma_{ij}^{(3)}(N)$; we approximate its best estimate with the average

$$\gamma_{ij}^{(3)}(N) = \frac{1}{\tilde{N}_{ij}} \sum_{k=1}^{\tilde{N}_{ij}} \gamma_{ij}^{(3),(k)}(N).$$

- We include the uncertainty on the average with the theory covariance matrix formalism (each instance $\gamma_{ij}^{(3),(k)}$ is seen as a nuisance parameter)

$$\Delta_m(ij, k) = T_m(ij, k) - \bar{T}_m \quad \text{cov}_{mn}^{(ij)} = \frac{1}{\tilde{N}_{ij} - 1} \sum_{k=1}^{\tilde{N}_{ij}} \Delta_m(ij, k) \Delta_n(ij, k).$$

- The total contribution to the theory covariance matrix is

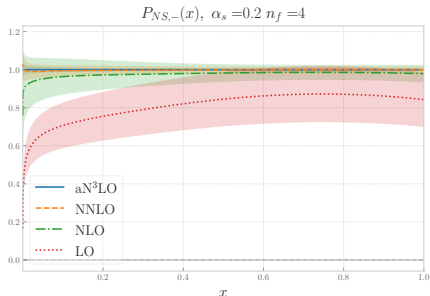
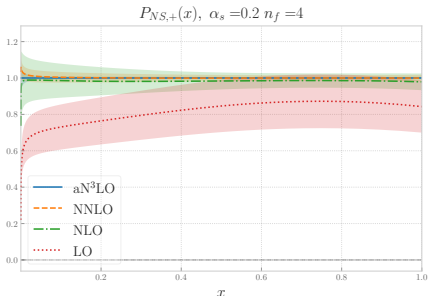
$$\text{cov}_{mn}^{\text{IHO}} = \text{cov}_{mn}^{(gg)} + \text{cov}_{mn}^{(gq)} + \text{cov}_{mn}^{(qq)} + \text{cov}_{mn}^{(qq)}$$

- The total theory uncertainty is the sum in quadrature of the IHO and MHO

$$\text{cov}_{mn}^{\text{tot}} = \text{cov}_{mn}^{\text{IHO}} + \text{cov}_{mn}^{\text{MHO}}$$

Splitting functions: non-singlet

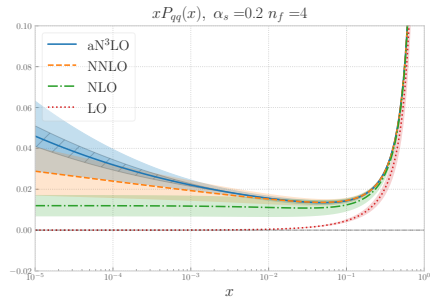
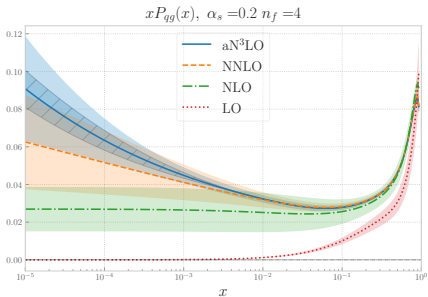
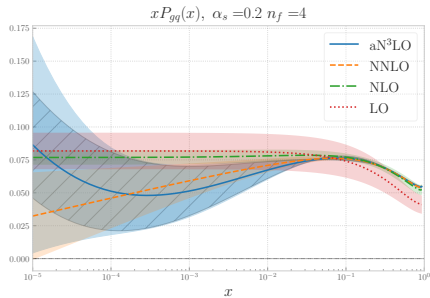
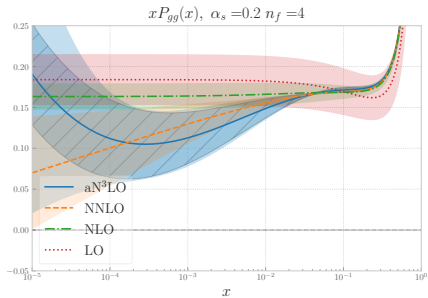
| | |
|--|------------------------------------|
| $G_1^{\text{ns},\pm}(N)$ | 1 |
| $G_2^{\text{ns},\pm}(N)$ | $\mathcal{M}[(1-x)\ln(1-x)](N)$ |
| $G_3^{\text{ns},\pm}(N)$ | $\mathcal{M}[(1-x)\ln^2(1-x)](N)$ |
| $G_4^{\text{ns},\pm}(N)$ | $\mathcal{M}[(1-x)\ln^3(1-x)](N)$ |
| $G_5^{\text{ns},\pm}(N)$ | $\frac{S_1(N)}{N^2}$ |
| $G_6^{\text{ns},\pm}(N)$ | $\frac{1}{(N+1)^2}$ |
| $G_7^{\text{ns},\pm}(N)$ | $\frac{1}{(N+1)^3}$ |
| $G_8^{\text{ns},+}(N), G_8^{\text{ns},-}(N)$ | $\frac{1}{(N+2)}, \frac{1}{(N+3)}$ |



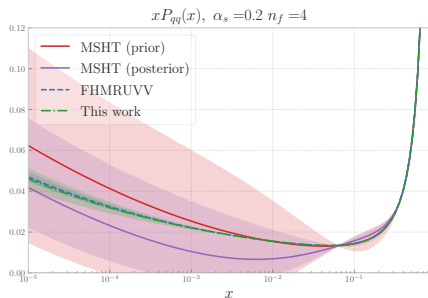
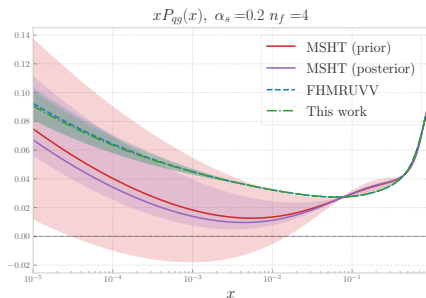
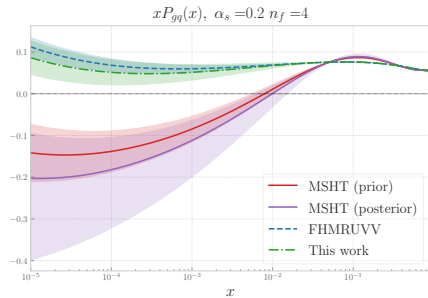
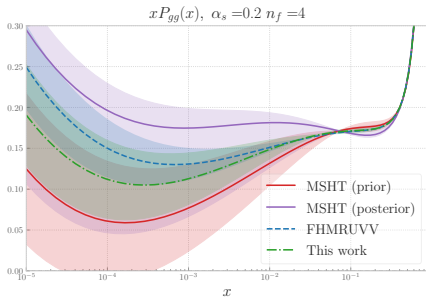
Splitting functions: singlet

| | | |
|---------------------------|--------------------------------------|--|
| | $G_1^{gg}(N)$ | $\mathcal{M}[(1-x)\ln^3(1-x)](N)$ |
| | $G_2^{gg}(N)$ | $\frac{1}{(N-1)^2}$ |
| $\gamma_{gg}^{(3)}(N)$ | $G_3^{gg}(N)$ | $\frac{1}{N-1}$ |
| | $\{H_1^{gg}(N), H_2^{gg}(N)\}$ | $\frac{1}{N^2}, \frac{1}{N^3}, \frac{1}{N^2}, \frac{1}{N+1}, \frac{1}{N+2}, \mathcal{M}[(1-x)\ln^2(1-x)](N), \mathcal{M}[(1-x)\ln(1-x)](N)$ |
| | $G_1^{gq}(N)$ | $\mathcal{M}[\ln^3(1-x)](N)$ |
| | $G_2^{gq}(N)$ | $\frac{1}{(N-1)^2}$ |
| $\gamma_{gq}^{(3)}(N)$ | $G_3^{gq}(N)$ | $\frac{1}{N-1}$ |
| | $\{H_1^{gq}(N), H_2^{gq}(N)\}$ | $\frac{1}{N^2}, \frac{1}{N^3}, \frac{1}{N^2}, \frac{1}{N+1}, \frac{1}{N+2}, \mathcal{M}[\ln^2(1-x)](N), \mathcal{M}[\ln(1-x)](N)$ |
| | $G_1^{qq}(N)$ | $\mathcal{M}[\ln^3(1-x)](N)$ |
| | $G_2^{qq}(N)$ | $\frac{1}{(N-1)^2}$ |
| $\gamma_{qq}^{(3)}(N)$ | $G_3^{qq}(N)$ | $\frac{1}{N-1} - \frac{1}{N}$ |
| | $G_{4,\dots,8}^{qq}(N)$ | $\frac{1}{N^2}, \frac{1}{N^3}, \frac{1}{N^2}, \frac{1}{N}, \mathcal{M}[\ln^2(1-x)](N)$ |
| | $\{H_1^{qq}(N), H_2^{qq}(N)\}$ | $\mathcal{M}[\ln(x)\ln(1-x)](N), \mathcal{M}[\ln(1-x)](N), \mathcal{M}[(1-x)\ln^3(1-x)](N)$ $\mathcal{M}[(1-x)\ln^2(1-x)](N), \mathcal{M}[(1-x)\ln(1-x)](N), \frac{1}{1+N}$ |
| | $G_1^{qq,ps}(N)$ | $\mathcal{M}[(1-x)\ln^2(1-x)](N)$ |
| | $G_2^{qq,ps}(N)$ | $-\frac{1}{(N-1)^2} + \frac{1}{N^2}$ |
| $\gamma_{qq,ps}^{(3)}(N)$ | $G_3^{qq,ps}(N)$ | $-\frac{1}{(N-1)} + \frac{1}{N}$ |
| | $G_{4,\dots,8}^{qq,ps}(N)$ | $\frac{1}{N^2}, \frac{1}{N^3}, \mathcal{M}[(1-x)\ln(1-x)](N)$ |
| | $\{H_1^{qq,ps}(N), H_2^{qq,ps}(N)\}$ | $\mathcal{M}[(1-x)^2\ln(1-x)^2](N), \mathcal{M}[(1-x)\ln(x)](N)$ $\mathcal{M}[(1-x)(1+2x)](N), \mathcal{M}[(1-x)x^2](N),$ $\mathcal{M}[(1-x)x(1+x)](N), \mathcal{M}[(1-x)](N)$ |

Splitting functions: singlet

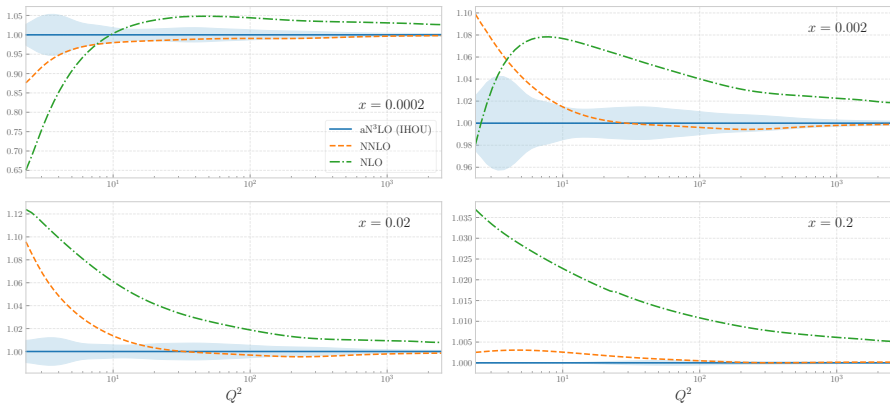


Splitting functions: singlet



A general-mass variable flavour number scheme at N3LO

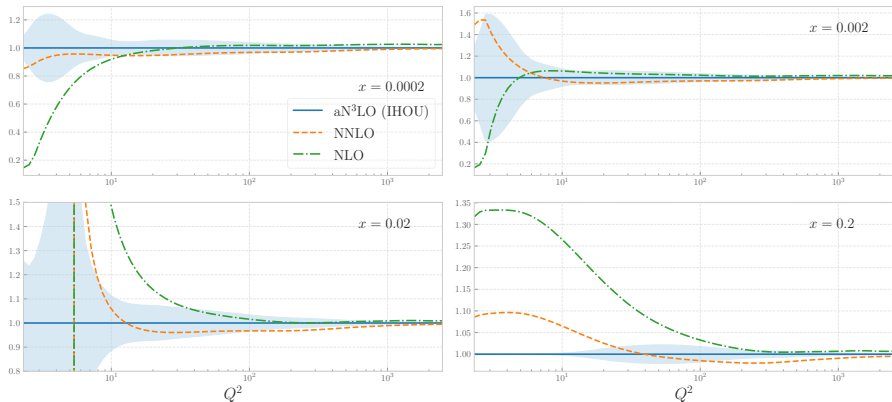
$F_2^{(\text{tot})}(x, Q^2)$, ratio to aN³LO



$$F_i^{\text{FONLL}} = F_i^{(n)}(x, Q^2, m_h^2) + F_i^{(n+1)}(x, Q) - F_i^{(n,0)}(x, \ln(Q^2/m_h^2)), \quad i = 2, L, 3$$

A general-mass variable flavour number scheme at N3LO

$F_2^{(c)}(x, Q^2)$, ratio to aN³LO

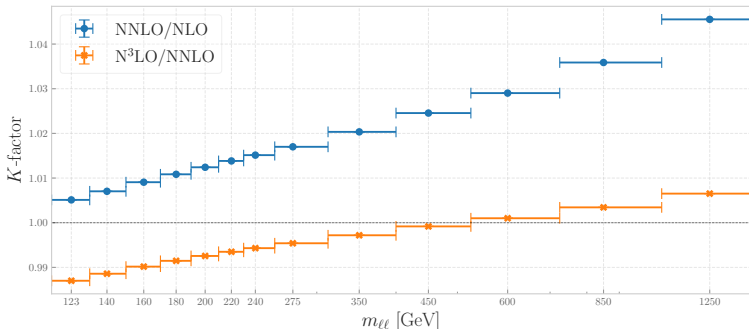


$$F_i^{\text{FONLL}} = F_i^{(n)}(x, Q^2, m_h^2) + F_i^{(n+1)}(x, Q) - F_i^{(n,0)}(x, \ln(Q^2/m_h^2)), \quad i = 2, L, 3$$

N3LO corrections to hadronic data

| Dataset | n_{dat} | Kin_1 | Kin_2 [GeV] | C -factor N ³ LO/NNLO |
|---|------------------|----------------------------------|-----------------------------------|---|
| ATLAS high-mass DY 7 TeV | 13 | $ \eta_\ell \leq 2.1$ | $116 \leq m_{\ell\ell} \leq 1500$ | $d\sigma/dm_{\ell\ell}$ |
| ATLAS Z 7 TeV ($\mathcal{L} = 35 \text{ pb}^{-1}$) | 8 | $ \eta_\ell, y_Z \leq 3.2$ | $Q = m_Z$ | $d\sigma/dm_{\ell\ell}$ ($66 < m_{\ell\ell} < 150$) |
| ATLAS Z 7 TeV ($\mathcal{L} = 4.6 \text{ fb}^{-1}$) | 39 | $ \eta_\ell, y_Z \leq 2.5, 3.6$ | $Q = m_Z$ | $d\sigma/dm_{\ell\ell}$ ($46 < m_{\ell\ell} < 116$) |
| ATLAS $\sigma_{W,Z}^{\text{tot}}$ 13 TeV | 3 | — | $Q = m_W, m_Z$ | σ |

Atlas high-mass DY 7 TeV



When N3LO corrections are not known, a 3pt MHOU is included in the cov. matrix

$$\text{cov}_{mn}^{\text{NNLO}} = \frac{1}{2} (\Delta_m(+)\Delta_n(+) + \Delta_m(-)\Delta_n(-))$$

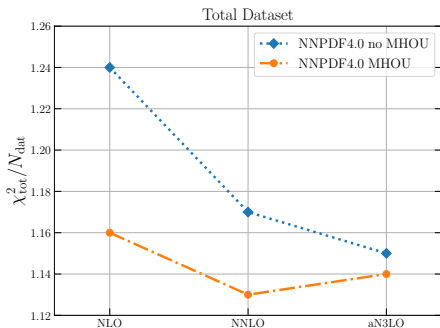
Fit quality

| Dataset | N_{dat} | NLO | | N_{dat} | NNLO | | N_{dat} | aN ³ LO | |
|-----------------------|------------------|-------------|-------------|------------------|-------------|-------------|------------------|--------------------|-------------|
| | | no MHO | MHO | | no MHO | MHO | | no MHO | MHO |
| DIS NC | 1980 | 1.30 | 1.22 | 2100 | 1.22 | 1.20 | 2100 | 1.22 | 1.20 |
| DIS CC | 988 | 0.92 | 0.87 | 989 | 0.90 | 0.90 | 989 | 0.91 | 0.92 |
| DY NC | 667 | 1.49 | 1.32 | 736 | 1.20 | 1.15 | 736 | 1.17 | 1.16 |
| DY CC | 193 | 1.31 | 1.27 | 157 | 1.45 | 1.37 | 157 | 1.37 | 1.36 |
| Top pairs | 64 | 1.90 | 1.24 | 64 | 1.27 | 1.43 | 64 | 1.23 | 1.41 |
| Single-inclusive jets | 356 | 0.86 | 0.82 | 356 | 0.94 | 0.81 | 356 | 0.84 | 0.83 |
| Dijets | 144 | 1.55 | 1.81 | 144 | 2.01 | 1.71 | 144 | 1.78 | 1.67 |
| Prompt photons | 53 | 0.58 | 0.47 | 53 | 0.76 | 0.67 | 53 | 0.72 | 0.68 |
| Single top | 17 | 0.35 | 0.34 | 17 | 0.36 | 0.38 | 17 | 0.35 | 0.36 |
| Total | 4462 | 1.24 | 1.16 | 4616 | 1.17 | 1.13 | 4616 | 1.15 | 1.14 |

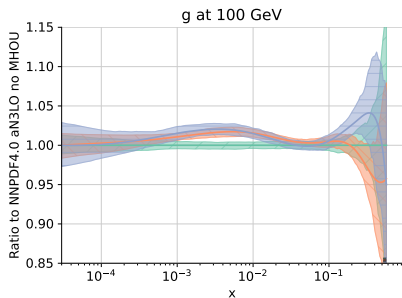
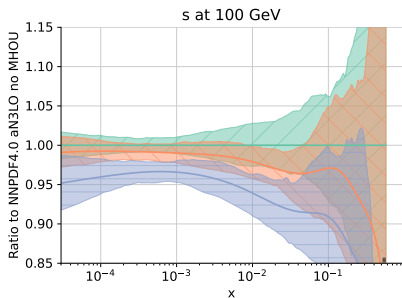
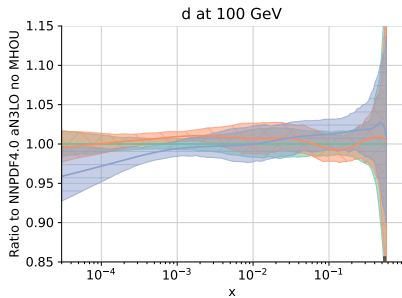
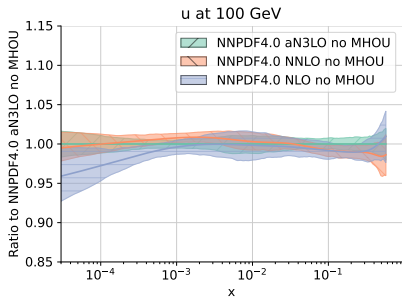
Fit quality improves with perturbative order

Fit quality almost independent from perturbative order when MHO are included

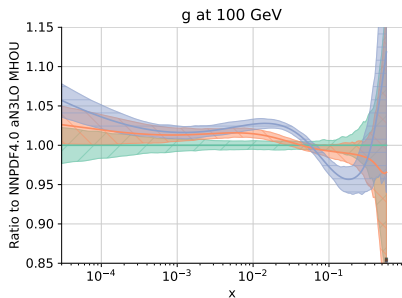
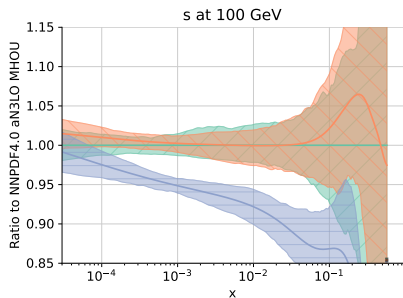
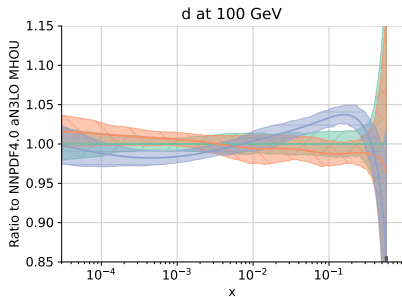
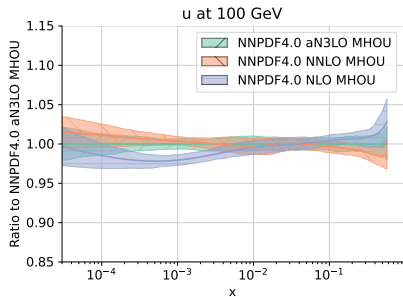
Data whose theoretical description is affected by large scale uncertainties are deweighted in favour of more perturbatively stable data



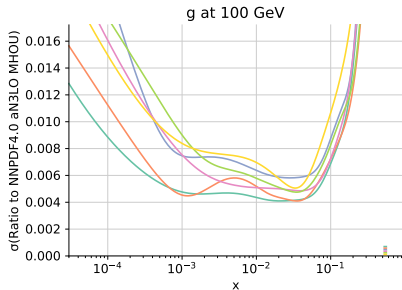
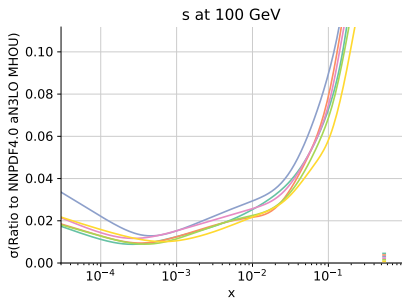
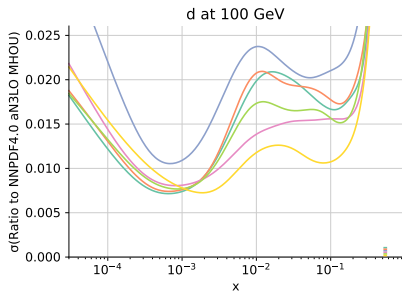
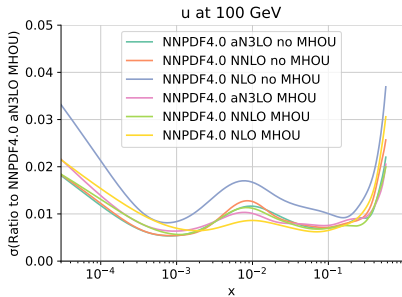
Perturbative dependence of PDFs: w/o MHOU



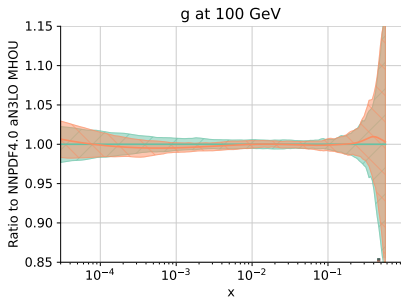
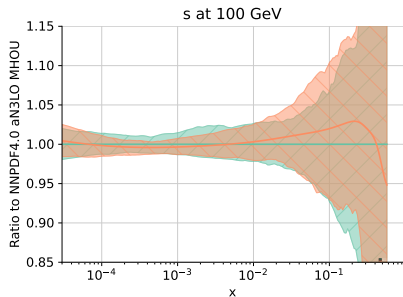
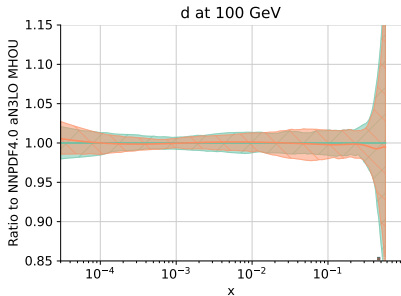
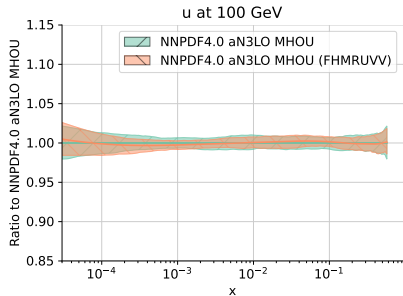
Perturbative dependence of PDFs: $w/$ MHOU



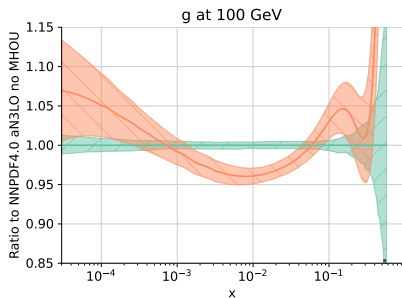
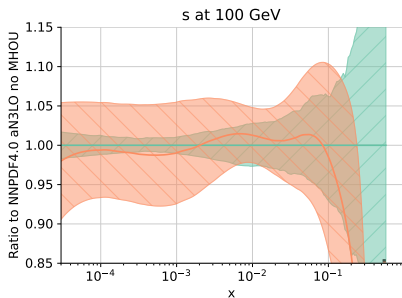
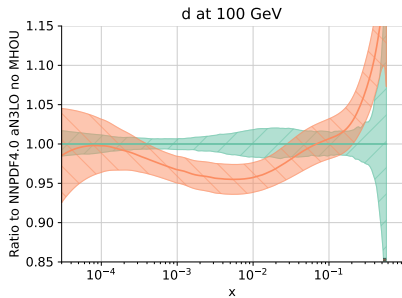
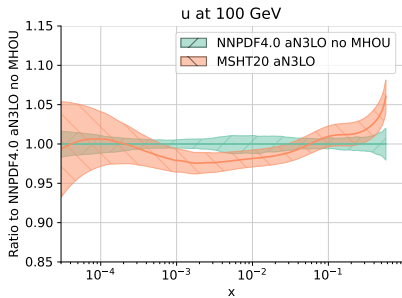
PDF uncertainties



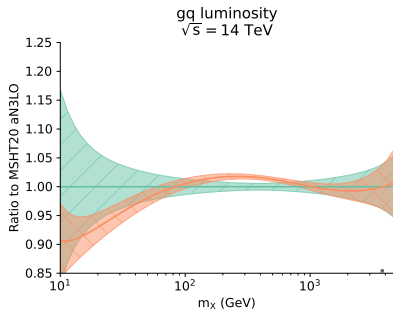
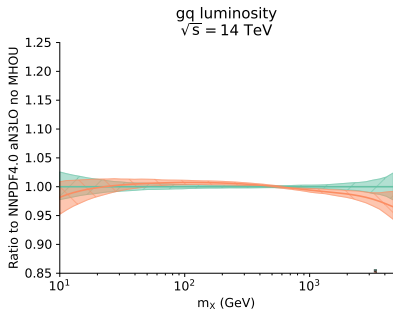
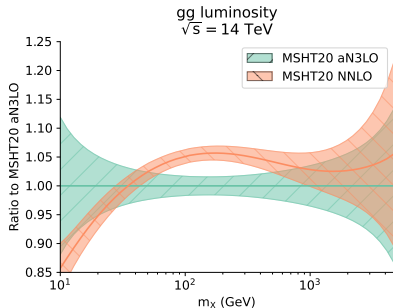
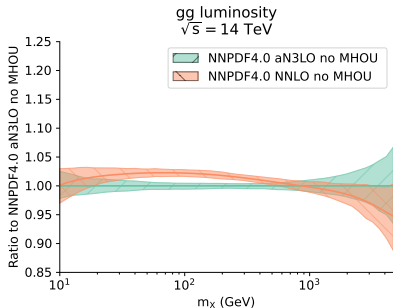
Dependence on splitting function parametrisation



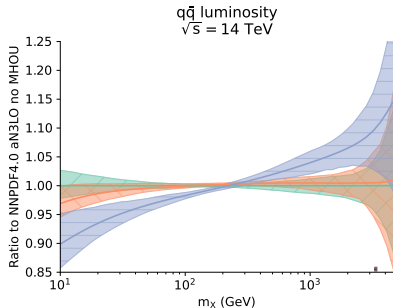
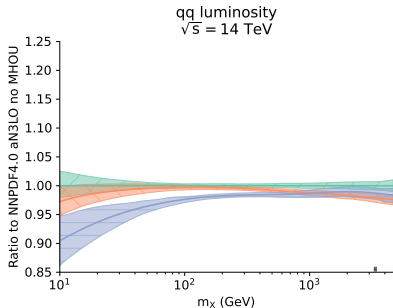
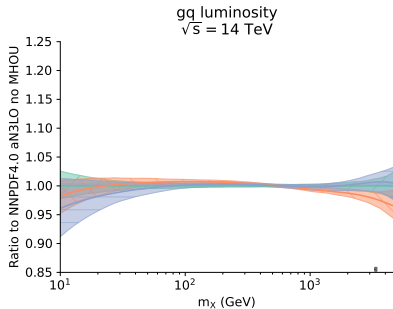
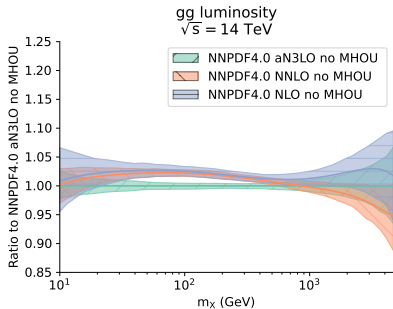
Comparison with MSHT20: PDFs



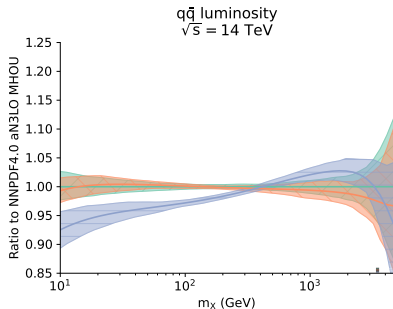
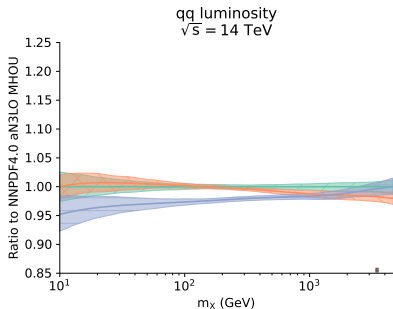
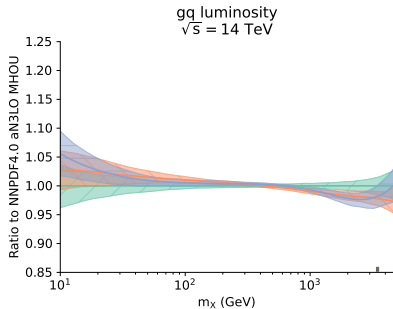
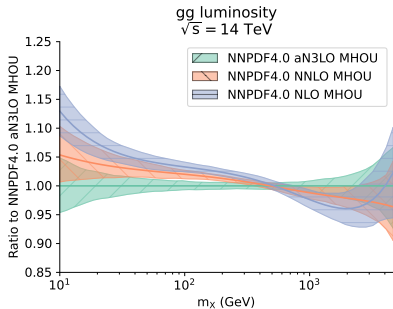
Comparison with MSHT20: partonic luminosities



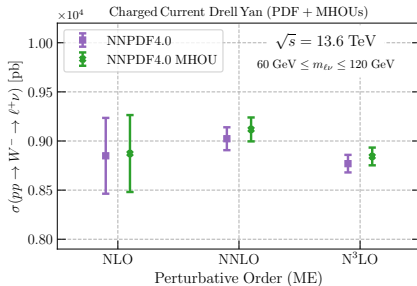
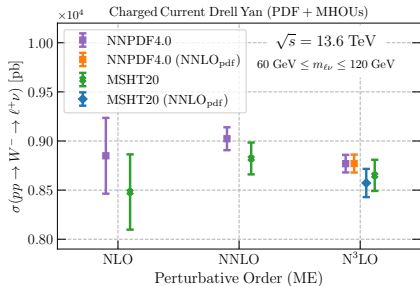
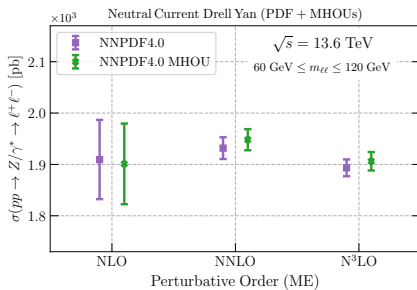
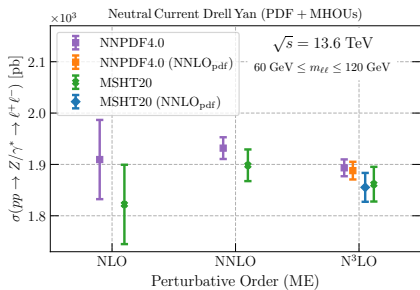
Partonic luminosities: w/o MHO



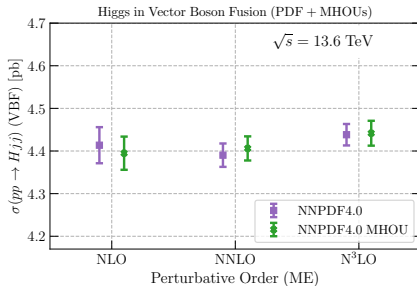
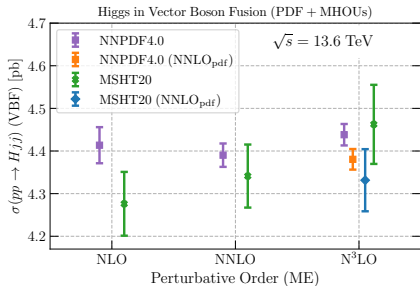
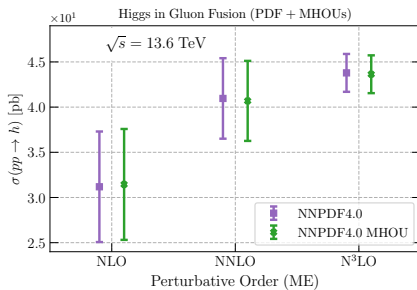
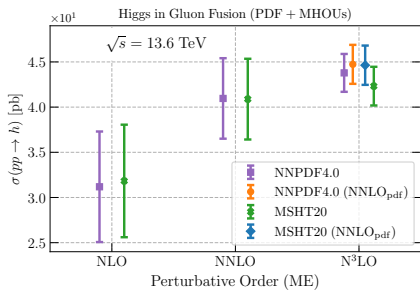
Partonic luminosities: w/ MHO



Inclusive cross sections: Drell–Yan

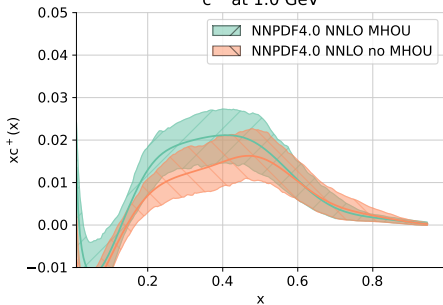


Inclusive cross sections: Higgs

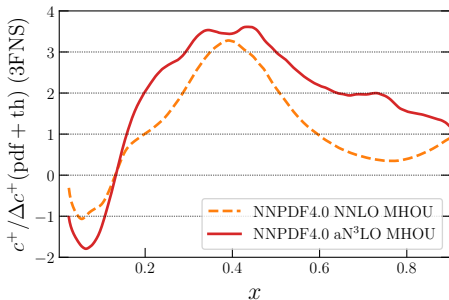
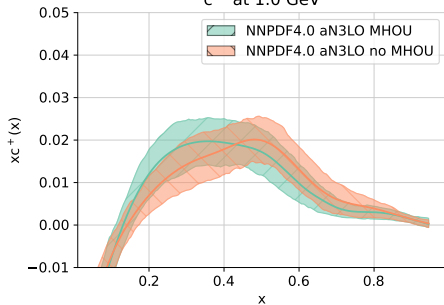


Implications for Intrinsic Charm

c^+ at 1.0 GeV



c^+ at 1.0 GeV



Intrinsic charm not affected
by aN3LO PDFs

Inclusion of MHOUs stabilises
its central value

Uncertainties remain unaffected by
aN3LO corrections and/or MHOUs

4. Conclusions

Summary

For all PDFs good perturbative convergence is observed, with differences decreasing as the perturbative order increases.

The effect of higher orders is negligible for quark PDFs, while it is sizeable for the gluon PDF.

The inclusion of MHOUs improves perturbative convergence, mostly by shifting central values at each order towards the higher-order result, by an amount that decreases with increasing perturbative order.

Upon inclusion of MHOUs the fit quality becomes independent of perturbative order
PDF uncertainties generally do not change.

The effect of MHOUs at $N^3\text{LO}$ is negligible for all PDFs, but for the gluon.

The impact of $N^3\text{LO}$ corrections on total cross-sections (e.g. Higgs in gg fusion) is very small on the scale of the PDF uncertainty.

Evidence for intrinsic charm is unchanged upon inclusion of $N^3\text{LO}$ corrections/MHOUs.

Check out our $aN^3\text{LO}$ and MHOU PDFs at
<https://nnpdf.mi.infn.it/nnpdf4-0-n3lo/>

Summary

For all PDFs good perturbative convergence is observed, with differences decreasing as the perturbative order increases.

The effect of higher orders is negligible for quark PDFs, while it is sizeable for the gluon PDF.

The inclusion of MHOUs improves perturbative convergence, mostly by shifting central values at each order towards the higher-order result, by an amount that decreases with increasing perturbative order.

Upon inclusion of MHOUs the fit quality becomes independent of perturbative order
PDF uncertainties generally do not change.

The effect of MHOUs at $N^3\text{LO}$ is negligible for all PDFs, but for the gluon.

The impact of $N^3\text{LO}$ corrections on total cross-sections (e.g. Higgs in gg fusion) is very small on the scale of the PDF uncertainty.

Evidence for intrinsic charm is unchanged upon inclusion of $N^3\text{LO}$ corrections/MHOUs.

Check out our $aN^3\text{LO}$ and MHOU PDFs at
<https://nnpdf.mi.infn.it/nnpdf4-0-n3lo/>

Thank you